

# Wave scattering and splitting by magnetic metamaterials

Alexander B. Kozyrev<sup>1</sup>, Chao Qin<sup>1</sup>, Ilya V. Shadrivov<sup>2</sup>,  
Yuri S. Kivshar<sup>2</sup>, Isaac L. Chuang<sup>3</sup>, and Daniel W. van der Weide<sup>1</sup>

<sup>1</sup>*Department of Electrical and Computer Engineering, University of Wisconsin-Madison,  
Madison, WI 53706, USA*

<sup>2</sup>*Nonlinear Physics Centre, Research School of Physical Sciences and Engineering,  
Australian National University, Canberra ACT 0200, Australia*

<sup>3</sup>*Massachusetts Institute of Technology, Cambridge, MA 02139, USA*

**Abstract:** We study experimentally propagation of electromagnetic waves through a slab of uniaxial magnetic metamaterial. We observe a range of novel phenomena including partial focusing and splitting into multiple transmitted beams. We demonstrate that while some of these experimentally observed effects can be described within the approximation of an effective medium, a deeper understanding of the experimental results requires a rigorous study of internal eigenmodes of the lattice of resonators.

© 2007 Optical Society of America

**OCIS codes:** (260.2110) Electromagnetic Theory; (999.9999) Metamaterials.

---

## References and links

1. D. R. Smith, W. J. Padilla, D. C. Vier, S. C. Nemat Nasser, and S. Schultz, "Composite medium with simultaneously negative permeability and permittivity," *Phys. Rev. Lett.* **84**, 4184–4187 (2000).
2. D. Schurig, J. J. Mock, B. J. Justice, S. A. Cummer, J. B. Pendry, A. F. Starr, and D. R. Smith, "Metamaterial electromagnetic cloak at microwave frequencies," *Science* **314**, 977–980 (2006).
3. E. Shamonina, V. A. Kalinin, K. H. Ringhofer, and L. Solymar, "Magnetoinductive waves in one, two, and three dimensions," *J. Appl. Phys.* **92**, 6252–6261 (2002).
4. D. R. Smith, D. Schurig, J. J. Mock, P. Kolinko, and P. Rye, "Partial focusing of radiation by a slab of indefinite media," *Appl. Phys. Lett.* **84**, 2244–2246 (2004).
5. D. R. Smith, P. Kolinko, and D. Schurig, "Negative refraction in indefinite media," *J. Opt. Soc. Am. B* **21**, 1032–1043 (2004).
6. D. Schurig and D. R. Smith, "Spatial filtering using media with indefinite permittivity and permeability tensors," *Appl. Phys. Lett.* **82**, 2215–2217 (2003).
7. D. R. Smith and D. Schurig, "Electromagnetic wave propagation in media with indefinite permittivity and permeability tensors," *Phys. Rev. Lett.* **90**, 077405–4 (2003).
8. A. A. Houck, J. B. Brock, and I. L. Chuang, "Experimental observations of a left-handed material that obeys Snell's law," *Phys. Rev. Lett.* **90**, 137401–4 (2003).
9. M. Hotta, M. Hano, and I. Awai, "Modal analysis of finite-thickness slab with single-negative tensor material parameters," *IEICE Trans. Electron.* **E89-C**, 1283 (2006).
10. M. S. Soskin and M. V. Vasnetsov, "Singular optics," in *Progress in Optics*, **42**, Ed. E. Wolf (North-Holland, Amsterdam, 2001), p.p. 219–276.
11. K. G. Balmain, A. A. E. Luttmann, P. C. Kremer, "Power flow for resonance cone phenomena in planar anisotropic metamaterials," *IEEE Trans. Antenn. Propag.* **51**, 2612–2618 (2003).
12. E. P. Brennan, A. Gardiner, A. G. Schuchinsky, V. F. Fusco, "Channelled waves in anisotropic mesh metamaterials," *IET Microw. Antennas Propag.* **1**, 56–64 (2007).
13. M. Gorkunov, M. Lapine, E. Shamonina, and K. H. Ringhofer, "Effective magnetic properties of a composite material with circular conductive elements," *Eur. Phys. J. B* **28**, 263–269 (2002).
14. C. A. Balanis, *Antenna Theory* (Wiley and Sons, Hoboken, New Jersey, 2005).
15. I. V. Shadrivov, A. N. Reznik, and Yu. S. Kivshar, "Magnetoinductive waves in arrays of split-ring resonators," *Physica B: Condensed Matter* **394**, 180–183 (2007).

## 1. Introduction

Recently, the study of microstructured metamaterials has received considerable attention in both physics and engineering. Metamaterials are artificial composites designed to exhibit the physical properties not usually found in nature. The first metamaterials were created by combining the lattices of split-ring resonators (SRRs) and long wires etched on dielectric substrates. Lattices of microstructured resonant elements are capable of producing strong magnetic and dielectric responses at microwave frequencies [1], and they exhibit unique properties such as negative refraction [1], sub-wavelength imaging, and cloaking [2]. Most of the available theoretical models describe the properties of these composite electromagnetic metamaterials within the framework of the effective medium approximation. The effective-medium approach is based on a simple averaging of the material response over the lattice of microelements, and it does not take into account any internal modes or resonances of the structure. Nevertheless, such eigenmodes exist in metamaterials composed of SRRs, and they are referred to as magnetoinductive (MI) waves (see, e.g., Ref. [3]). Existence of such waves can significantly modify the metamaterial response as compared to the effective medium theory.

In this paper we study, both experimentally and numerically, the effect of magnetoinductive waves on the transmission properties of uniaxial composite metamaterials consisting of the lattice of SRRs. This type of metamaterial was first studied by Smith *et al.* [4, 5, 6, 7], and it was called *an indefinite medium*, since the tensor of effective magnetic permeability has the main components of the opposite signs. Such media demonstrate interesting effects such as negative refraction [5], partial focusing [4], and spatial beam filtering [6] all previously described by the effective medium approach. In contrast to those earlier works, here we report a series of novel effects which *cannot be described within the effective medium theory*.

More specifically, we excite a slab of a magnetic metamaterial by a monopole antenna and analyze the beam structure behind the slab. Although the scale of the composite constituents remain *much smaller* than the wavelength of the excitation radiation (one of the major requirements for the applicability of the averaged theories), we observe that an effective medium fails to describe some of the observed effects, including the beam multiple splitting. We develop a numerical algorithm for describing the lattices of SRRs in terms of inductively interacting resonant loops, and confirm qualitatively the major effects observed in experiments.

## 2. Experimental setup

A slab of magnetic metamaterial is assembled by stacking dielectric substrates with metallic SRR structures with the same dimensions as the structures used in Ref. [8], and is constructed of 50  $\mu\text{m}$  thick tin-plated copper on a 0.5 mm thick GML-1000 circuit board substrate. The unit cell of the SRR lattice is 6 mm in  $x$  direction by 3.3 mm in  $z$  (see Fig. 1). Each board has 3 unit cells in  $z$  and 41 unit cells in  $x$ , and the corresponding total physical dimensions are 10 mm by 246 mm. Boards are stacked together, so that the unit cell size in  $y$  direction is 0.55 mm. We have measured two samples having 20 and 25 layers, corresponding to the metamaterial thicknesses in  $y$  direction of 10 mm and of 12.5 mm, respectively.

To measure the electromagnetic field scattering on our samples, the magnetic metamaterial slab was placed into a parallel plate waveguide similar to one used in Ref. [8]. The planes of SRRs are aligned perpendicular to the parallel plate surfaces. The input antenna is placed at the midpoint of the lower plate, 6 mm from the metamaterial slab, in front of the central SRR unit cell, and it consists of a bare center conductor of 1.26 mm diameter and 8.5 mm long of semi-

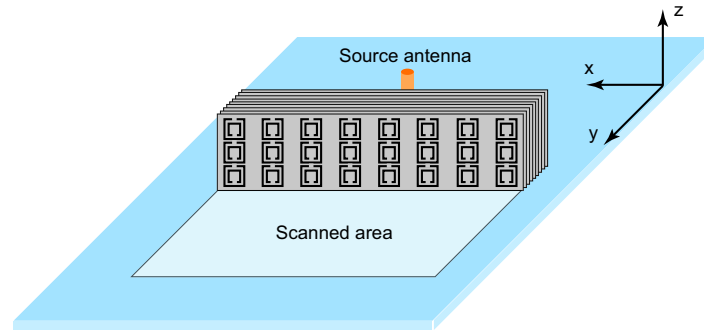


Fig. 1. Schematic of the experimental setup for measurement of the wave scattering. SRR geometry is identical with one used in Ref. [8]

rigid coaxial cable. The antenna is positioned perpendicular to the bottom plate. An identical antenna is placed in the center of the top plate, and is used as receiver antenna for raster scan of the fields in the horizontal plane. The measurements are performed in an anechoic chamber to minimize ambient noise. The input antenna is excited at -5 dBm using an Agilent E8364A vector network analyzer. The output antenna is connected to the network analyzer as well, and measurements of the electric field inside the waveguide are evaluated in terms of the magnitude and phase of  $S_{21}$  between the source and receiver antenna. Due to the two-dimensional nature of the parallel plate waveguide, as well as symmetry of our sample, the electric field in the scanned area is expected to remain polarized mainly perpendicular to the plane of the plates (i.e., in  $z$ -direction).

### 3. Experimental results

The electric field is mapped within a rectangular area of 20 cm by 10 cm (see schematic in Fig. 1), with the smaller dimension oriented in the direction of propagation (along  $y$ ). The area being scanned is 1.85 cm from the input antenna. The apparatus was configured to measure the magnitude and phase of the electric field with a step size of 0.25 cm (3200 points in total). The frequency was scanned over a range from 6 GHz to 14 GHz, with frequency steps of 0.1 GHz.

In the case of 20-layer metamaterial we observed near-field patterns created by the TE guided mode propagating along strongly anisotropic metamaterial in the transverse ( $x$ ) direction [9](from 6 GHz to 8.6 GHz, as seen in the video attached to the Fig. 2), and a partial focusing, qualitatively similar to the phenomena described in Ref. [4], (from 8.6 GHz to 10.6 GHz). Typical structure of the transmitted beam in partial focusing regime is shown in Fig. 2 (a,d), where we plot the magnitude and the phase of the electric field measured at 10 GHz. However, above 10.7 GHz, in contrast to the effective medium theory prediction, the central focus splits into two collimated beams (areas of intensive field) that propagate at an angle relative to  $y$ . The magnitude of the signal transmitted through the slab of SRR metamaterial, measured at 10.8 GHz, is shown in Fig. 2 (b, e). Upon an increase in frequency, the “beams” gradually separate from each other and the angle between them increases, while the intensity of the field in the “beam” areas decreases (see Fig. 2 (c,f)). The “beams” move out of the scanned area completely above 12.5 GHz. Phase distributions (Fig. 2) behind the metamaterial slab have discontinuities that correlate with the shape of the lobes in the corresponding magnitude plots, indicating generation of vortices (see, e.g., [10]).

The beam splitting, or spatial filtering, that we observed looks similar to the resonant cone formation in planar anisotropic metamaterial (grid of L-C elements and TL segments) [11, 12].

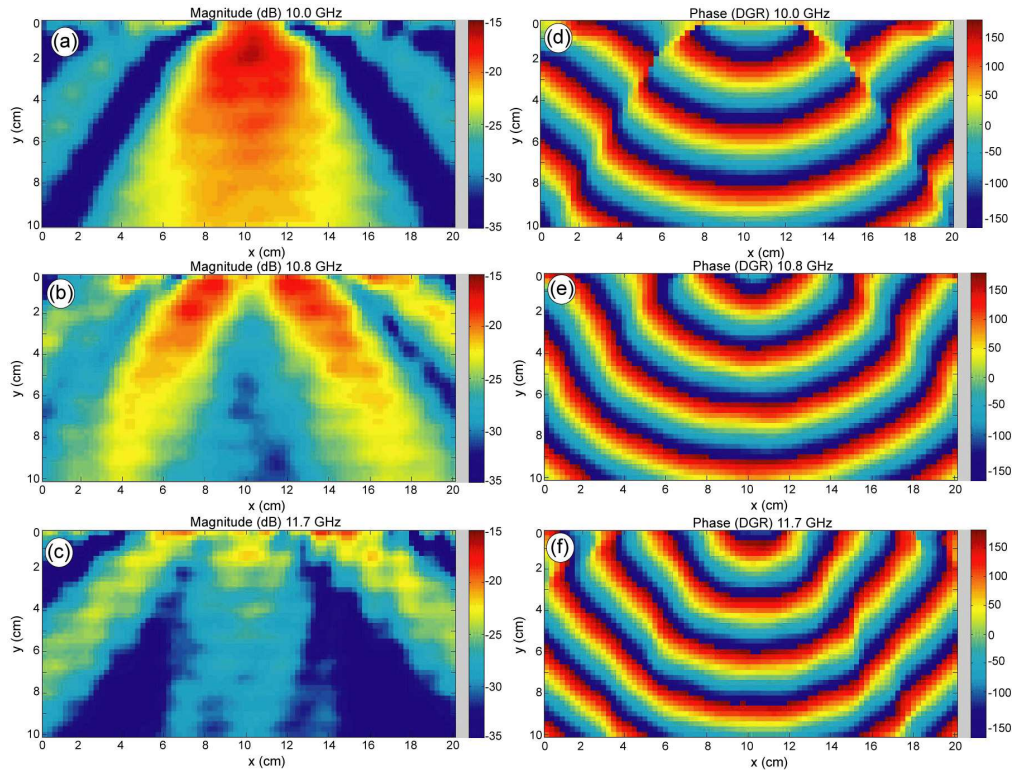


Fig. 2. Field structure behind the 20-layer magnetic metamaterial slab. Shown are magnitude (a, b, c) and phase (d, e, f) of the transmitted signal, for three different frequencies, 10 GHz, 10.8 GHz and 11.7 GHz.

However, the physical origin of these phenomena is completely different. Balmain et. al. [11] observed beam splitting inside the planar anisotropic metamaterial while we observed the beam splitting in the air behind the metamaterial slab.

Reference measurement of the field structure in the waveguide without magnetic metamaterial confirmed the cylindrical shape of the wave radiated by the antenna and also demonstrated that the attenuation seen in the field is not significant. The field intensity in the beam regions behind the metamaterial is comparable, or even higher than the field intensity in the same area in the reference measurements.

The field structure behind the metamaterial slab depends significantly on the slab thickness. In the case of the 25-layer metamaterial we observed partial focusing in the higher frequency range (from 10.3 GHz to 11.8 GHz) compared to the case of 20-layer structure. Moreover, there is no splitting of the focus into two side beams upon an increase in the frequency above 11.8 GHz. However, we did observe splitting of the central focus into three separate focal points at lower frequencies. Thus, the field structure at 8.2 GHz shown in Fig. 3 (a) has three distinct foci, the central beam and the two side beams behind these foci. With an increase in frequency, the distance between the side foci decrease in conjunction with the angle between the side beams (compare the field structure at 8.2 GHz and 8.8 GHz in Fig. 3) and they finally collapse at the center giving rise to a "partial focus" upon further increase in frequency. This collapse is also accompanied by the rise of two other side beams. With further increase in the frequency, the angle between these beams increases, and they move towards the boundaries of the scanned

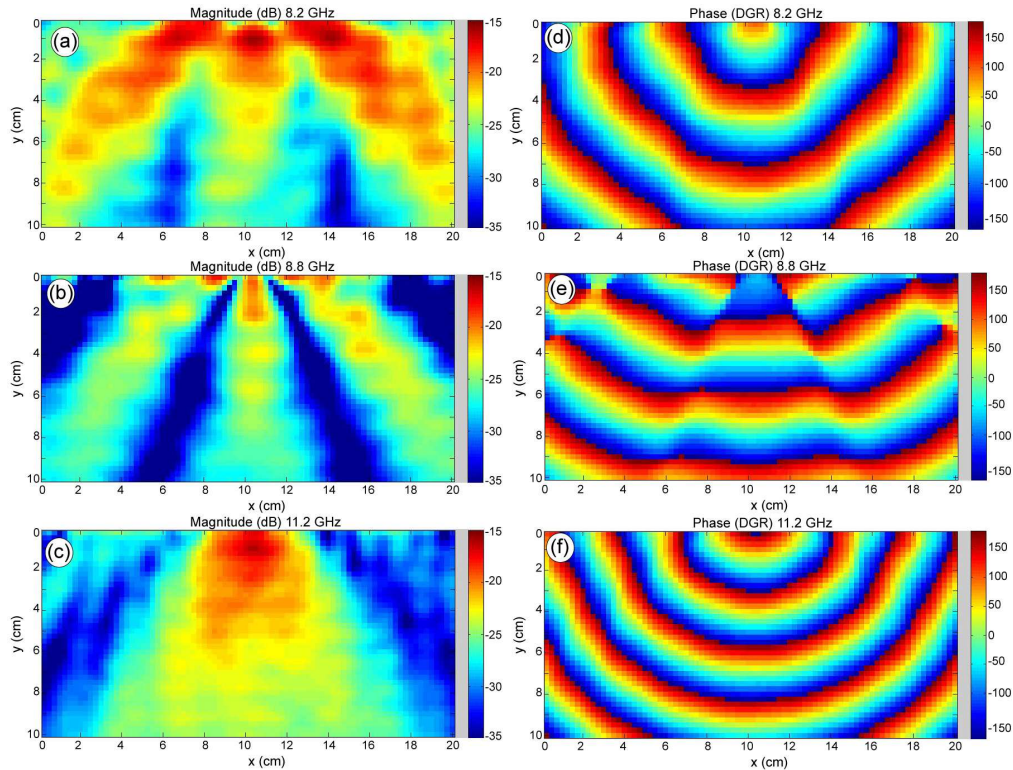


Fig. 3. Field structure behind the 25-layer magnetic metamaterial slab. Shown are magnitude (a, b, c) and phase (d, e, f) of the transmitted signal, for three different frequencies, 8.2 GHz, 8.8 GHz and 11.2 GHz.

area and then disappear.

#### 4. Theoretical approach

##### 4.1. Effective medium approach

In order to understand the field distributions observed experimentally, we carried out HFSS simulations employing effective medium approximation. According to this approach the magnetic metamaterial was modeled as anisotropic medium with the permeability tensor having non-zero diagonal components. Typical field distributions inside and behind metamaterial calculated for  $\mu_{xx} = \mu_{zz} = 1$  and  $\mu_{yy} = -1.5$  are presented in Fig. 4. Comparison of the field distribution behind the metamaterial slab as presented in Fig. 4 to the measured field structure shown in Fig. 2(a) and in corresponding video, shows that the effective medium approach can be used to explain the generation of the TE guided mode (Fig. 4 (a)) and partial focusing (Fig. 4 (b)). This is in full agreement with the results of Ref. [4]. However, the calculated field structure qualitatively preserves its features in the frequency range from 8.6 GHz till 14 GHz, and for wide range of possible values of  $\mu_{yy} < 0$ . Thus, the beam splitting observed in our experiment behind the magnetic metamaterial slab cannot be predicted by this theory.

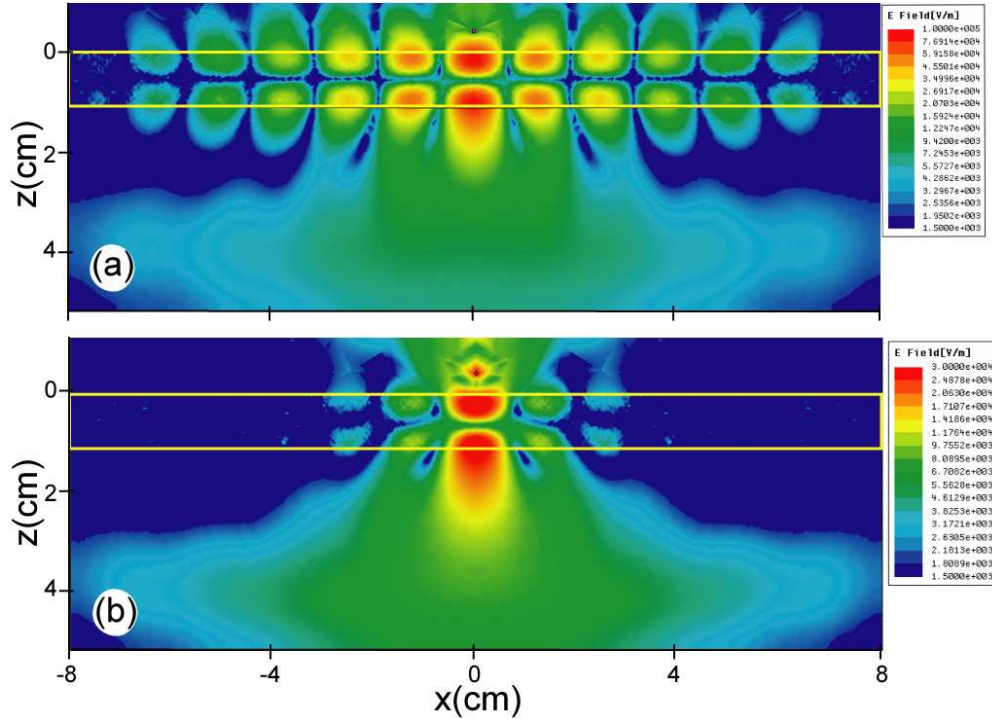


Fig. 4. Simulated field distributions ( $|E|$ ) generated by the current source located at the distance 4mm from the slab. Shown are results for (a)  $f = 8.5$  GHz, and (b)  $f = 9$  GHz.

#### 4.2. Magnetoinductive waves in SRR array

In order to overcome the restrictions of the effective medium approach and to explain the experimental results on beam splitting, we study the wave scattering by an array of interacting magnetic dipoles in quasi-static approximation. Such arrays support *magnetoinductive waves* [3]. First, we calculate the dispersion of such waves, assuming  $\exp(i\omega t)$  time dependence. Corresponding isofrequency curves are shown in Fig. 5. Due to the strong axial coupling of the resonators in our magnetic metamaterial, the MI waves exist in a wide frequency range below the resonant frequency of the individual resonator  $\omega_0$  (approximately from  $0.65\omega_0$  to  $1.05\omega_0$ ). Isofrequency curves in the range  $0.65\omega_0 < \omega < 0.71\omega_0$  are qualitatively similar to the hyperbolic dispersion curves obtained from an effective medium theory [4]. However, the isofrequency curves for  $0.71\omega_0 < \omega < 1.05\omega_0$  have no analogs in that approach. The dramatic change in the shape of isofrequency curves that occurs at  $\omega/\omega_0 \approx 0.71$  would require components of permeability perpendicular to the axis of SRRs to be negative which can not be justified within the effective medium approximation.

Next, we study numerically the excitation of MI waves and their effect on the field structure behind the metamaterial slab. Each SRR was modeled as a resonant circuit and the currents  $I_n$  in each resonator were calculated using the following equation [13]:

$$Z_n I_n + \sum_{n'} Z_{nn'} I_{n'} = \mathcal{E}_n. \quad (1)$$

Here  $Z_n$  is self-impedance of the  $n$ -th SRR,  $Z_{nn'}$  is mutual impedance of the resonators with the numbers  $n$  and  $n'$ , and  $\mathcal{E}_n = i\omega\mu_0 S H_n$  is the external electromotive force, where  $S$  is the area of the SRR, and  $H_n$  is the component of the magnetic field perpendicular to the  $n$ -th resonator.

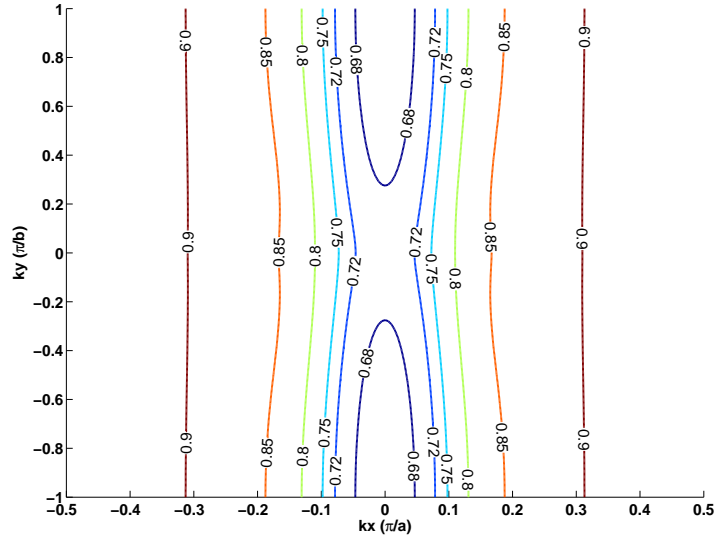


Fig. 5. Isofrequency curves of magnetoinductive waves.  $a, b$  are structural periods along  $x$  and  $y$  directions. Marked are the normalized frequencies,  $\omega/\omega_0$ .

In our geometry, we approximate radiation of our source antenna with dipole radiation formulas [14], and calculate  $\mathcal{E}_n$  for each resonator. Then, we solve Eq. (1) for the currents in each resonator. The total field created in our structure is calculated as  $E_z = E_{sz} + \sum E_{nz}$ , where  $E_{sz}$  is the  $z$ -component of the source field, and  $E_{nz}$  is the  $z$ -component of the electric field radiated by the  $n$ -th SRR. The field emitted by each SRR was approximated by the field of a small loop antenna [14].

In our simulations, we use the parameters taken from the experiment. The resonant frequency of an individual resonator is 10 GHz [8], self-impedance of the resonator is approximated by a single-resonance model, and mutual inductance of square resonators is calculated as a superposition of mutual inductances of interacting straight sections of the resonators. Results of numerical simulations are shown in Fig. 6 for two different frequencies. Field distribution shown in Fig. 6 (a) relates to the case of TE guided mode excitation and it is in a good agreement with experimental results (video attached to the Fig. 2) and with the results of HFSS simulations shown in Fig. 4 (a). Furthermore, simulated field structure given in Fig. 6 (b) confirms that the excitation of magnetoinductive waves is responsible for the complicated field pattern generated behind the metamaterial slab. As discussed above, dispersion curves corresponding to this case do not have reasonable analogs within the effective medium theory.

Our simulations describe the experimentally observed phenomena only qualitatively. Apparently, the use of the quasi-static model for interacting SRRs (through mutual inductances  $Z_{nm'}$ ) is not accurate enough in the case when the size of the resonator is just ten times smaller than the free-space wavelength, as was first noticed in Ref. [15] for one-dimensional magnetoinductive waves. The model of lattices of *interacting dipoles* [16] is more accurate. Indeed, if we compare our isofrequency surfaces shown in Fig. 5 with those obtained in Ref. [16], we can see that the quasistatic model does not describe all modes of the structure. However, the main conclusion of both the theories is the same, namely that the effective medium approximation is not valid for all frequencies.

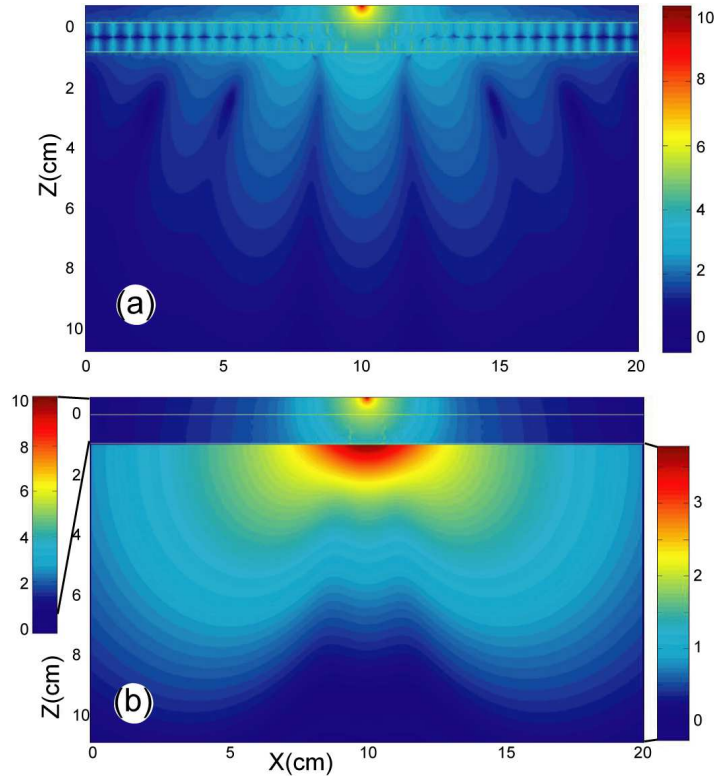


Fig. 6. Electric field intensity  $|E_z|$  distribution for 20-layer metamaterial slab in logarithmic scale: (a)  $\omega = 7.5GHz$  and (b)  $\omega = 10.5GHz$ . Yellow lines show edges of the magnetic metamaterial slab. Field below the slab in (b) is plotted in different color scale compared to the rest of the figure in order to enhance representation. Corresponding colorbars are presented on the figures.

## 5. Conclusions

We have observed experimentally the waveform splitting into two or multiple beams after the propagation of electromagnetic waves through a slab of a magnetic metamaterial. We have emphasized that this effect can not be described by a standard theoretical approach based on the effective-medium approximation when a slab of microstructured composite is characterized by some effective permittivity and permeability. Instead, we have suggested that the transmission properties of metamaterials can be affected significantly by their internal resonances, such that the multiple beam formation observed in the experiments can be attributed to the excitation of magnetoinductive waves. From the other side, by incorporating tunable or nonlinear components into metamaterial structure would allow achieving novel tunable functionalities for steering and advanced beam control.

## Acknowledgments

This work was supported by the Air Force Office of Scientific Research (AFOSR) through the MURI program (grant F49620-03-1-0420). IS and YK acknowledge a support from the Australian Research Council and thank P. Belov for useful discussions. IS acknowledges travel



support from the Australian Academy of Science. Authors thank Alan Bettermann for proof-reading the manuscript.